Electrocatalytic Reactions of a Manganese−Pyrylium Complex

Michael J. Shaw* and Jaime Mertz

Department of Chemistry, Box 1652, Southern Illinois University Edwardsville, Edwardsville, Illinois 62026

Received May 21, 2002

A salt of a metal−pyrylium σ-complex, pentacarbonyl-3-(2-methoxy-5,6-diphenylpyrylium)-manganese(I) tetrafluoroborate (**1BF$_4$**), has been prepared by the action of $Mn(CO)_5BF_4$ on methyl propiolate and diphenylacetylene. The pyrylium complex shows unusual resistance to electrophilic cleavage of the Mn−C bond by H^+ and a low aptitude for migratory insertion reactions. The complex was studied by spectroscopic, voltammetric, and controlled potential electrolysis methods. **1BF$_4$** displays two ligand-based one-electron reductions ($E_1° = -1.33$ V, $E_{pc,2} = -2.41$ V vs Fc), the first of which is Nernstian. Its reactivity is enhanced by one-electron reduction, and it undergoes subsequent dimerization in THF ($k_{273K} = 285\ M^{-1}\ s^{-1}$) and CH_2Cl_2 ($k_{273K} = 260\ M^{-1}\ s^{-1}$) and a CO dissociation equilibrium ($K \approx 1.4 \times 10^5$, $k = 0.7\ s^{-1}$). In the presence of triphenylphosphine, a slow electrocatalytic CO-substitution reaction occurs for which a mechanism and rate constants have been determined by digital simulation. When **1**BF_4 is reduced in the presence of $HSnPh_3$ and a proton donor, another electrocatalytic process results, presumably forming H_2 at the electrode surface.

Introduction

Transition-metal complexes that promote the homogeneous electrocatalytic generation of hydrogen from protic substrates have garnered increasing interest in recent years.[1,2] These systems are of interest because of the need for technologies that produce energy sources such as H_2 on demand. The mechanism of H_2 production often involves reduction and subsequent protonation of a metal complex to generate a metal-hydride.[1] This hydride ligand reacts with H^+ to regenerate the precursor complex and H_2. Such reactivity has many parallels to the models of the NAD/NADH system, which have received considerable attention in recent years[3] and which have proven very amenable to electrochemical study.[4] Both metal-hydrides and NADH serve as H^- donors to electrophilic substrates other than H^+. Recently, reports that metal ions such as Mg^{2+} serve as cofactors to bind a substrate molecule in place during H-transfer from NADH analogues[5] have captured our attention.

A metal complex designed so that a transition-metal atom is in close proximity to the active site of an NADH analogue might display cooperative reactivity between the two sites.[6] We have recently prepared several metal−pyrylium complexes that fit this description.[7] Like pyridinium ions, many pyrylium ions can accept H^- equivalents at the para-position.[8] The resulting 4H-pyrans are known to be hydride donors.[9] Pyrylium ions are also easier to reduce than the corresponding pyridinium ions, owing to the greater electronegativity of the oxygen atom. This property should make catalytic activity available at more benign potentials.[10] However, cationic hydrocarbyl groups such as pyridinium or pyrylium bound to the metal via a M−C σ-bond are very

* Corresponding author. E-mail: michsha@siue.edu. Fax: 618 650-3556.

(1) Divisek, J.; Schmitz, H.; Steffen, B. *Electrochim. Acta* **1994**, *39*, 1723. (b) Bhugun, I.; Lexa, D.; Savéant, J. M. *J. Am. Chem. Soc.* **1996**, *118*, 3982. (c) Grass, V. Lexa, D.; Savéant, J.-M. *J. Am. Chem. Soc.* **1997**, *119*, 7526, and references therein.

(2) (a) Zassinovich, G.; Mestroni, G.; Gladiali, S. *Chem. Rev.* **1992**, *92*, 1051. (b) Fache, F.; Schulz, E.; Tommasino, M. L.; Lemaire, M. *Chem. Rev.* **2000**, *100*, 2159. (c) Bullock, R. M.; Voges, M. H. *J. Am. Chem. Soc.* **2000**, *122*, 12594. (d) Luan, L. Song, J.-S.; Bullock, R. M. *J. Org. Chem.* **1995**, *60*, 7170. (e) Troutman, M. V.; Appella, D. H.; Buchwald, S. L. *J. Am. Chem. Soc.* **1999**, *121*, 4916.

(3) (a) Eisner, U.; Kuthan, J. *Chem. Rev.* **1972**, *72*, 1. (b) Stout, D. M.; Meyer, A. I. *Chem. Rev.* **1982**, *82*, 223. (c) Fukuzumi, S. *Advances in Electron-Transfer Chemistry*; Mariano, P. S., Ed.; JAI Press: Greenwich, CT, 1992; pp 67−175. (d) Pestovsky, O.; Bakac, A.; Espenson, J. H. *J. Am. Chem. Soc.* **1998**, *120*, 13422. (e) Pestovsky, O.; Bakac, A.; Espenson, J. H. *Inorg. Chem.* **1998**, *37*, 1616. (f) Marcinek, A.; Adamus, J.; Huben, K.; Gebicki, J.; Bartczack, T. J.; Bednarek, P.; Bally, T. *J. Am. Chem. Soc.* **2000**, *122*, 437.

(4) (a) Anne, A.; Fraoua, S.; Moiroux, J.; Savéant, J.-M. *J. Am. Chem. Soc.* **1996**, *118*, 3938. (b) Anne, A.; Fraoua, S.; Grass, V.; Moiroux, J.; Savéant, J.-M. *J. Am. Chem. Soc.* **1998**, *120*, 2951. (c) Mairanovskii, S. G. *Catalytic and Kinetic Waves in Polarography*; Plenum: New York, 1968; pp 245−261.

(5) (a) Ohno, A.; Oda, S.; Ishikawa, Y.; Yamazaki, N. *J. Org. Chem.* **2000**, *65*, 6381. (b) Cheng, J.-P.; Lu, Y.; Zhu, X.; Mu, L. *J. Org. Chem.* **1998**, *63*, 6108.

(6) Some intermolecular reactivity of this type is known; see: (a) Lo, H. C.; Buriez, O.; Kerr, J. B.; Fish, R. H. *Angew. Chem., Int. Ed.* **1999**, *38*, 1429. (b) Rudler, H.; Audouin, M.; Parlier, A.; Martin-Vaca, B.; Goumont, R.; Durand-Réville, R.; Vaissermann, J. *J. Am. Chem. Soc.* **1996**, *118*, 12045−12058

(7) Shaw, M. J.; Light, S.; Mertz, J.; Ripperda, S. Manuscript in preparation.

(8) (a) Kuthan, J.; Sebek, P.; Böhn, S. *Adv. Heterocycl. Chem.* **1995**, *62*, 19. (b) Ohkata, K.; Akiba, K.-Y. *Adv. Heterocycl. Chem.* **1996**, *65*, 283.

(9) Pozharskii, A. F. *Heterocycles in Life & Society; An Introduction to Heterocyclic Chemistry & Biochemistry & the Role of Heterocycles in Science, Technology, Medicine & Agriculture*: Wiley: New York, 1997; and references therein

(10) (a) Balaban, A. T.; Dinculescu, A.; Dorofeenko, G. N.; Fischer, G.; Koblik, A. V.; Mezheritskii, V. V.; Schroth, W. *Pyrylium Salts: Syntheses Reactions and Physical Properties: Advances in Heterocyclic Chemistry Supplement 2*; Academic Press: New York, 1982. (b) Farcasiu, D.; Balaban, A. T.; Bologa, U. L. *Heterocycles* **1994**, *37*, 1165. (c) Ohkata, K.; Akiba, K.-Y. *Adv. Heterocycl. Chem.* **1996**, *65*, 283.

10.1021/om020405n CCC: $22.00
Publication on Web 06/22/2002

rare.[11,12] Despite the large number of pyrylium compounds known, few σ-bonded organometallic pyrylium complexes have been prepared and investigated.[12,13] This oversight is surprising in light of the utility of pyrylium salts in organic synthesis and their applications as dyes, laser dyes, photosensitizers, and corrosion-inhibiting additives in paints.[9,10] They also have a rich redox chemistry, undergoing reduction to form stable radicals, dimers, or pyrans, depending on steric factors and on the reducing agent. The coupling of this redox chemistry to the recognized properties of transition-metal complexes has the potential to yield systems with useful physical and chemical properties. For example, such ligands would be expected to be less electron-rich than neutral ligands and are expected to have properties consistent with this relative lack of electron density.

In this paper, we outline the preparation of a new organometallic pyrylium complex and its electrochemistry under conditions where migratory insertion and electrophilic M−C bond cleavage is possible. We present herein evidence that such cationic ligands are attached to the metal via robust M−C σ-bonds which resist electrophilic cleavage and migratory insertion reactions. Furthermore, this compound displays the ability to undergo two types of electrocatalytic reaction depending on the reaction conditions, and we will demonstrate the utility of square wave voltammetry to supplement the information that is available by cyclic voltammetry in this investigation.

Results and Discussion

(1) Synthesis of Pentacarbonyl-3-(2-methoxy-5,6-diphenylpyrylium)manganese(I) ($\mathbf{1}^+\mathbf{BF_4}$). The ability of metal cations to condense organic compounds into cyclic structures is well-documented.[14] In particular, the ability of Fp^+ (Fp = η^5-$C_5H_5(CO)_2Fe$) to condense acetylenic esters with alkenes to form cyclic products including six-membered lactone rings[15] prompted Legzdins to determine that $[CpM(NO)_2]^+$ salts (Cp′ = Cp, Cp*; M = Cr, Mo, W) form the corresponding lactones as the sole products.[12] Using an alkyne in the place of an alkene resulted in the formation of the pyrylium complexes instead of lactones.

We have found that $[Mn(CO)_5]BF_4$[16,17] and $[Mn(CO)_5]PF_6$ also mediate the condensation of methyl propiolate and diphenylacetylene to form an organometallic pyrylium complex (eq 1).

Further studies into which metal cations mediate this process and the overall mechanism of this reaction are underway, but it seems reasonable to suggest that the first step of the reaction involves η^2-coordination of the methyl propiolate to the metal center, as originally proposed by Rosenblum for the preparation of Fp-lactone complexes.[15] There have been recent reports of other electrophile-mediated cyclization reactions to prepare pyrylium salts.[18]

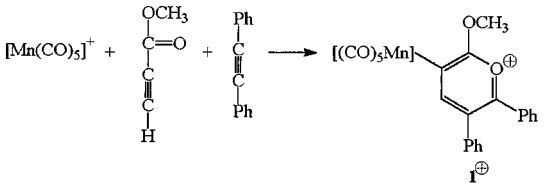

(1)

The physical properties of $\mathbf{1}^+$ are consistent with the positive charge being distributed around the pyrylium ring. For example, $\mathbf{1}^+$ has bands in its IR spectrum at 2135, 2084, 2040, and 2017 cm^{-1}, which may be compared to those of $Mn(CO)_5CH_3$ (2110, 2030 (shoulder), 2010, and 1986 cm^{-1}) and $Mn(CO)_5I$ (2125, 2043, 2012, and 1982 cm^{-1}). The overall intensity pattern and the shift to higher wavenumbers for $\mathbf{1}^+$ indicate a similar geometry at a slightly less electron-rich Mn center, as expected for a species with a cationic hydrocarbyl ligand. The ^1H NMR spectra reveal signals due to the H atom on the 4-position of the pyrylium ring at 8.45 ppm in $\mathbf{1}^+$. This highly deshielded signal confirms that the positive charge primarily resides on the pyrylium ring, leaving a relatively uncharged metal center. The pyrylium ligand in $\mathbf{1}^+$ also seems to be the primary redox site, as expected from a comparison of pyrylium and $Mn(CO)_5R$ redox potentials (vide infra). This compound is air stable in the solid state and in $CDCl_3$ solution for several days.

The positive charge on the pyrylium ring has a strong influence on the reactivity of $\mathbf{1}^+$. Most $Mn(CO)_5R$ (R = alkyl, aryl) complexes undergo CO-insertion reactions when treated with external ligands and undergo immediate Mn−C bond cleavage in the presence of H^+.[19] ^1H NMR experiments reveal that complex $\mathbf{1}^+$, on the other hand, is unaffected by equimolar HBF_4 for at least 2 days in $CDCl_3$. Similarly, the ^1H NMR and ^{31}P NMR spectra of solutions that contain $\mathbf{1}^+$ and 2 equiv of PPh_3 undergo no change over a period of a week, conditions where a neutral $Mn(CO)_5R$ complex would undergo migratory insertion to form a phosphine-substituted acyl complex. The robust Mn−pyrylium bond in $\mathbf{1}^+$ can be explained by the fact that the positively charged ligand is unlikely to be a good nucleophile. Thus, its bond to the metal center is not subject to electrophilic cleavage by H^+, nor does it display a migratory aptitude, since it appears to be not nucleophilic enough to attack a coordinated CO ligand.

Electrochemistry of Complex $\mathbf{1}^+$. In CH_2Cl_2 at 0 °C, complex $\mathbf{1}^+$ displays two cathodic features by cyclic voltammetry as shown in Figure 1. Similar electrochemistry is observed in THF. The first reduction occurs at $E^{o\prime} = -1.33$ V vs Fc, and its anodic return wave is visible at scan rates >50 mV/s. This feature appears to be due to a one-electron process with fast charge transfer due to the $\mathbf{1}^{+/0}$ couple as indicated by comparison of the ΔE_p values to those of the ferrocene standard (e.g., both are 70 mV at 200 mV/s) and bulk coulometry

(11) Garnovskii, A. D.; Sadimenko, A. P. *Adv. Heterocycl. Chem.* **1998**, *72*, 1.
(12) Legzdins, P.; McNeil, W. S.; Vessey, E. G. *Organometallics* **1992**, *11*, 2718.
(13) Ohe, K.; Mike, K.; Yokoi, T.; Nishino, F.; Uemura, S. *Organometallics* **2000**, *19*, 5525, and references therein.
(14) (a) Lautens, M. Klute, W.; Tam, W. *Chem. Rev.* **1996**, *96*, 49. (b) Fruhauf, H.-W. *Chem. Rev.* **1997**, *97*, 523. (c) Cotton, F. A.; Wilkinson, G.; Murillo, C. A.; Bochman. *Advanced Inorganic Chemistry*, 6th ed.; Wiley: New York, 1999, and references therein. (d) Collman, J. P.; Hegedus, L. S.; Norton, J. R.; Finke, R. G. *Principles and Applications of Organotransition Metal Chemistry*; University Science Books: Mill Valley, 1987; and references therein.
(15) Rosenbloom M.; Scheck, D. *Organometallics* **1982**, *1*, 397.
(16) Reger, D. L.; Coleman *J. Organomet. Chem.* **1977**, *131*, 153.
(17) Chaffee, S. C.; Sutton, J. C.; Babbitt, C. S.; Mayer, J.; Guy, K. A.; Pike, R. D.; Carpenter, G. B. *Organometallics*, **1998**, *17*, 5586.
(18) Tovar, J. D.; Swager, T. M. *J. Org. Chem.* **1999**, *64*, 6499.
(19) Johnson, M. D. *Acc. Chem. Res.* **1978**, *11*, 57.

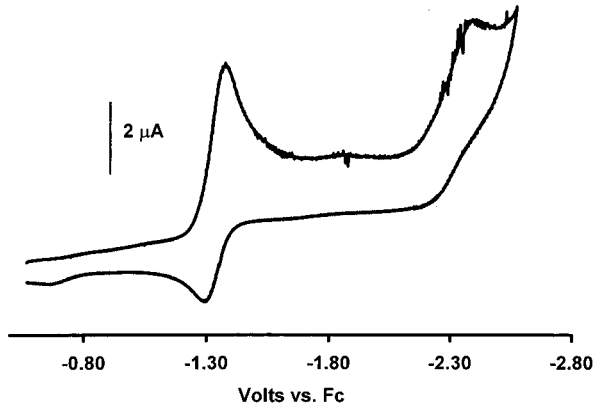

Figure 1. CV of 1.0 mM **1**BF_4 at 200 mV/s, in 0.15 M NBu_4PF_6 in CH_2Cl_2 at 0 °C at a 1 mm Pt disk electrode.

Table 1. Electrochemical Data for 1^+ in CH_2Cl_2/ 0.15 M NBu_4PF_6 at 0 °C

scan rate (mV/s)	$\Delta E_p(\mathbf{1}^{+/0})$ (mV)	I_{pa}/I_{pc} ($\mathbf{1}^{+/0}$)	$E_{pc}(\mathbf{1}^{0/-})$ (V)
50	82	0.46	−2.36
100	84	0.53	−2.38
200	82	0.62	−2.41
400	91	0.72	−2.45
800	102	0.81	−2.48
1600	122	0.87	−2.53

experiments (vide infra). The chemical reversibility (I_{pa}/I_{pc}) for this feature is over 0.9 in cyclic voltammograms (CVs) recorded at scan rates in excess of 3200 mV at 0 °C, but at lower scan rates, the reduction is less chemically reversible (Table 1). The reversibility improves as the temperature is lowered, so that at −45 °C the first reduction appears completely Nernstian at scan rates faster than 400 mV/s. At temperatures over 0 °C, the follow-up reaction for this reduction seems to be primarily a relatively slow dimerization process, most likely involving coupling of the neutral pyranyl radicals. A second reduction due to the $\mathbf{1}^{0/-}$ couple occurs at E_{pc} = −2.41 V vs Fc at 200 mV/s in CH_2Cl_2 (Table 1). It is chemically irreversible at 3200 mV/s and lower scan rates above 0 °C. This couple is the same height as the $\mathbf{1}^{+/0}$ couple and is presumably due to another one-electron process.

These two redox processes are most likely ligand based. Pyrylium ions are known to undergo one-electron reversible reductions in the range −0.6 to −1.29 V vs Fc.[10b] This range is consistent with $\mathbf{1}^+$ possessing a rather electron-rich pyrylium ligand as the primary redox site. It is also known that $Mn(CO)_5X$ (X = alkyl, aryl, trialkylstanyl, halide) complexes undergo two-electron reductions to form the pentacarbonylmanganese(−I) anion and that the reduction potentials show little dependence on the identity of ligand X.[20] In our hands, the most easily reduced complex of this group, namely, $Mn(CO)_5I$, undergoes two closely spaced irreversible reductions at −1.93 and −2.12 V vs Fc at 0° in CH_2Cl_2. The IR data indicate a similar amount of electron density on the metal center in $\mathbf{1}^+$ and $Mn(CO)_5I$, so it is unlikely that the metal's redox potential would change by 600 mV to more positive values because of substitution by an iodide ligand by the pyrylium group. It can also be argued that the one-electron nature of the second redox process in $\mathbf{1}^+$ is inconsistent with the usually observed two-electron behavior of $Mn(CO)_5X$ complexes, which produce the well-known $[Mn(CO)_5]^-$ anion upon reduction. The presence of this anionic species is clearly evident in scans of $Mn(CO)_5I$ as an anodic peak at −0.62 V vs Fc, which appears following reduction of the starting iodide complex. This wave is conspicuously absent from scans of $\mathbf{1}^+$, which means that little or no $[Mn(CO)_5]^-$ is produced under these conditions.

Table 2. Rate Constants for Dimerization of $\mathbf{1}^0$ in THF

T (K)	rate constant (M^{-1} s^{-1})
295	950
273	285
251	142
233	80

The reduction of $\mathbf{1}^+$ was studied in some detail in CH_2Cl_2 at 0 °C. When the method of Nicholson and Shain[21] is used to extract first-order rate constants from CVs recorded between 50 and 1600 mV/s, the k values increase systematically with increasing scan rate for both THF and CH_2Cl_2 by a total of 300%. Since dimerization of pyranyl radicals is a well-known consequence of the reduction of pyrylium ions, simulations were performed using DIGISIM[22] taking into account a second-order follow-up reaction. This approach led to a good match between the experimental and simulated voltammograms when k_1 = 260 M^{-1} s^{-1}. Under these conditions, simulated reversibilities were within the experimental reversibilities for each of the 5 scan rates considered (50−1600 mV/s). At high concentrations, a wave due to the dimerized product appears at E_{pc} = −1.8 V vs Fc. This peak is barely visible in 1.0 mM solutions (Figure 1) but can be clearly seen in 5.0 mM solutions. This wave decreases in intensity with increasing scan rate in a manner consistent with a second-order reaction with the same rate constant as for the process that diminishes the amount of $\mathbf{1}^0$ at the electrode surface. It also diminishes when the temperature is lowered and disappears upon addition of an H atom source such as $HSnPh_3$. The latter reagent indicates that the radical dimerization process is slower than atom-abstraction processes for $\mathbf{1}^0$.

The reduction of $\mathbf{1}^+$ was also examined in THF over a 67° temperature range. The reversibility of the $\mathbf{1}^{+/0}$ couple at 20 and 0 °C was analyzed by the method of Nicholson and again resulted in first-order rate constants that were dependent on scan rate. Simulation (with DIGISIM) of this EC process as a second-order reaction results in good agreement (<6% difference) between the observed and the simulated reversibilities for scan rates where I_{pa}/I_{pc} < 0.85 (i.e., 50−800 mV/s at 22 °C). At 0° there is good agreement between the rate constants found in THF (285 M^{-1} s^{-1}) and CH_2Cl_2 (260 M^{-1} s^{-1}). Furthermore, this wave is less chemically reversible at higher concentrations, as expected for a second-order process. Rate constants were found for other temperatures (Table 2), but there also seems to

(20) (a) Dessy, R. E.; Stary, F. E.; King, R. B.; Waldrop, M. *J. Am. Chem. Soc.* **1988**, *88*, 471. (b) Morris, M. D. *Adv. Electroanal. Chem.* **1974**, *7*, 80, and references therein.

(21) Nicholson, R. S.; Shain, I. *Anal. Chem.* **1964**, *36*, 706. (b) Shain, I. *Anal. Chem.* **1966**, *38*, 1406.

(22) Rudolph, M.; Reddy. D. P.; Feldberg, S. W. *Anal. Chem.* **1994**, *66*, 589A.

be another process that diminishes the amount of $\mathbf{1}^0$ present at the electrode surface, which becomes relatively important at low temperatures. The presence of another process can be inferred from the curvature of the van't Hoff plot of these data. At high temperature, the associative dimerization reaction is important, but at lower temperatures, a CO dissociation may predominate (vide infra).

In both THF and CH_2Cl_2 a chemically irreversible anodic peak is present after the first reduction wave is scanned at slow rates (Figure 2). This feature appears at $E_{pa} = -0.39$ V vs Fc (200 mV/s), and it diminishes in intensity as the scan rate is raised, with the concomitant increase in chemical reversibility of the $\mathbf{1}^{+/0}$ couple. This peak is ascribed to the oxidation of the dimer to re-form $\mathbf{1}^+$. Electrolysis of a 0.60 mM solution of $\mathbf{1}^+BF_4$ with a carbon electrode at −1.45 V vs Fc at −45 °C results in the passage of 1 Faraday-equivalent of charge, which confirms the one-electron nature of this process. After electrolysis, the solution displays an irreversible cathodic peak at −2.31 V vs Fc and the previously observed irreversible anodic peak at −0.39 V vs Fc. Scanning of this anodic peak results in enhancement of the signal due to residual $\mathbf{1}^+$ present, thereby indicating that the electrolysis product can be converted back into the starting material on the CV time scale. Regeneration of the starting material following oxidation of the product dimer is expected, given the known behavior of other bulky dimeric pyrans and dihydropyridines.[10]

Further characterization of the electrolytically generated product revealed it to consist of a mixture of species resulting from 2,2′-, 2,4′-, and 4,4′-coupling of the pyranyl radicals. The electrolysis product was extracted with hexane from the supporting electrolyte after removal of the CH_2Cl_2 under reduced pressure. This solution displayed ν(CO) IR bands at 2125, 2069, 2045, 2033, 2008, 1964, and 1746 cm^{-1}. Significantly, the IR data do not match $Mn_2(CO)_{10}$ (ν(CO)'s at 2045, 2011, 1978 cm^{-1}), which is the product of reduction of $Mn(CO)_5Br$ and $Mn(CO)_5I$, a fact that lends further support to the organic ligand as the site of electron transfer. However, when the hexane was removed and this sample was dissolved in $CDCl_3$, the ^1H NMR spectrum revealed five significant peaks between 3.0 and 3.8 ppm. From a consideration of the ^1H signals expected for the uncomplexed pyrans, four methoxy resonances are expected for a mixture of the 2,2′-, 2,4′-, and 4,4′-coupled products, and the final peak in this region is appropriate for the 4−4′ CH group. Smaller peaks in this region may indicate that some coupling also occurs through the 6-position. Additionally, a peak at 4.65 ppm and a peak at 9.65 ppm are suggestive of the 2,4- and the 2,2-coupled products, respectively, along with phenyl resonances. The NMR results suggest that dimerization occurs best through the sterically available 2- and 4-positions.

Synthetic attempts to prepare and separate these isomers have been unsuccessful. These products react with chromatographic supports such as silica gel. While reduction of $\mathbf{1}^+PF_6$ with Zn in DME yields a similar mixture of isomers as judged by IR and ^1H NMR, chromatography on silica gel affords a small amount of an impure product. This substance had IR bands at 2122, 2068, 2027, 2000, 1951, 1750, and 1691 cm^{-1} and

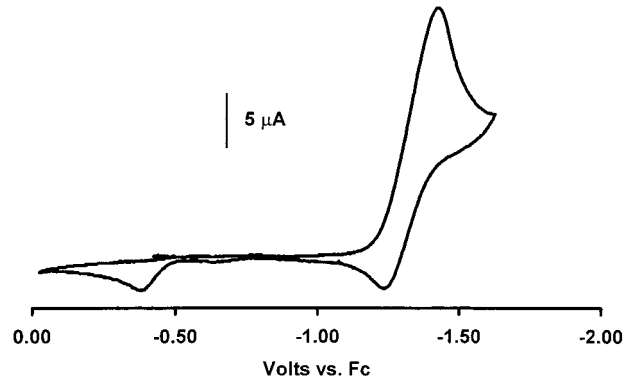

Figure 2. CV of 5.0 mM $\mathbf{1}BF_4$ at 200 mV/s, in 0.10 M NBu_4PF_6 in THF at 22 °C at a 1 mm Pt disk electrode.

NMR peaks at 2.8, 3.9, 7.1−8.2, 8.4, and 8.8 ppm, and electrospray MS indicates a parent ion at 903 *m/z*, which corresponds to $C_{45}H_{29}O_{14}Mn_2$. This formula can be rationalized by loss of CO with the gain of an OH group. Although attempts to crystallize this substance have thus far been unsuccessful, it is clearly a product of a dimerization reaction and may be due to an OH^--induced ring-opening reaction in which the acyclic ligand displaces a carbonyl ligand from the metal.

On the basis of the second-order kinetics arising from the CV investigation, the electrochemical and spectroscopic data of the product species generated by electrolysis, the synthetic efforts, and the known reduction chemistry of pyrylium ions, it is reasonable to conclude that $\mathbf{1}^+$ dimerizes upon reduction, through the sterically accessible 2- and 4-position on the ring, as shown in eq 2.

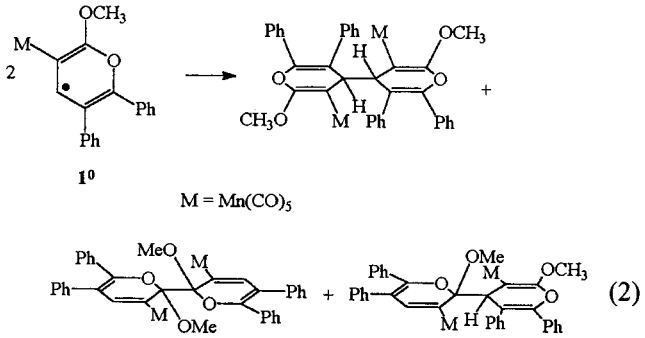

(2)

Electrochemistry in the Presence of PPh_3. Because of the known migratory insertion chemistry of $RMn(CO)_5$ complexes, the redox behavior of $\mathbf{1}^+$ in the presence of external ligands was investigated. CO substitution in this system fits a dissociative electrocatalytic mechanism where $(OC)_4(PPh_3)$Mn(methoxydiphenylpyrylium), $\mathbf{3}^+$, forms at the electrode surface. No evidence for migratory insertion was found. This CO-dissociation equilibrium is likely the other process that complicates the kinetics of the EC dimerization of $\mathbf{1}^+$ at low temperature.

In Figures 3−5 are displayed CVs and square wave voltammograms (SWVs) recorded in the presence of triphenylphosphine and simulations of these data. These data were analyzed using ESP 2.4[23] because this program can simulate SWV data in addition to CV data.

(23) ESP 2.4 by Dr. Carlo Nervi is available at http://lem.ch.unito.it/ without charge for academic use.

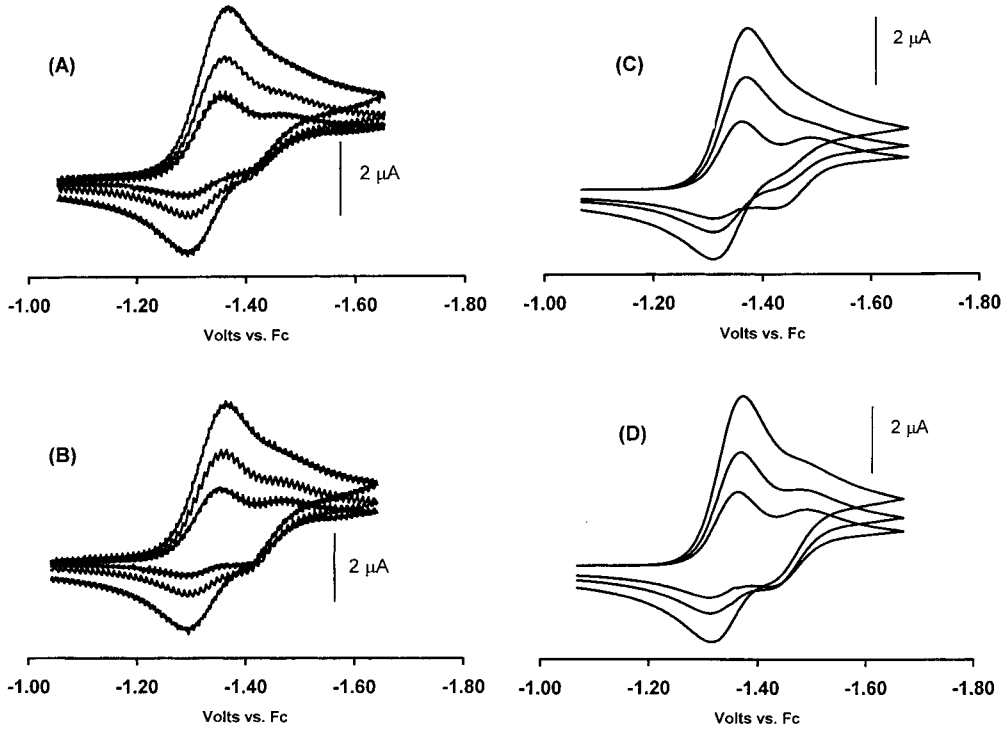

Figure 3. CVs of 1.3 mM **1**BF_4 at 50, 100, and 200 mV/s: (A) 1.3 mM PPh_3; (B) 13 mM PPh_3; (C) simulation, 1.3 mM PPh_3; (D) simulation, 13 mM PPh_3.

The CV simulations thus obtained were in good agreement with DIGISIM simulations using the same mechanism and parameters. A number of mechanisms were considered, but only the following explained the gross and subtle features of each CV and SWV recorded regardless of the phosphine concentration. While the theory of square wave voltammetry is well-developed[24] and there are a number of tools to simulate SWV data, its use in determining electrode mechanisms in organometallic chemistry has been sparse, even though it offers complementary information to CV.

$$\mathbf{1}^+ + e^- \rightleftharpoons \mathbf{1}^0 \qquad E° = -1.33 \text{ V vs Fc} \qquad (3)$$

$$\mathbf{1}° + \mathbf{1}° \rightarrow \mathbf{2} \qquad k_1 = 2.6 \times 10^2 \text{ M}^{-1}\text{ s}^{-1} \qquad (4)$$

$$\mathbf{1}^0 \rightleftharpoons \mathbf{4} + \text{CO}$$
$$k_2 = 0.7 \text{ s}^{-1},\ k_{-2} = 1.0 \times 10^4 \text{ M}^{-1}\text{ s}^{-1} \qquad (5)$$

$$\mathbf{4} + \text{PPh}_3 \rightarrow \mathbf{3}^0 \qquad k_3 = 1.0 \times 10^3 \text{ M}^{-1}\text{ s}^{-1} \qquad (6)$$

$$\mathbf{3}^+ + e^- \rightleftharpoons \mathbf{3}^0 \qquad E° = -1.41 \text{ V vs Fc} \qquad (7)$$

Reaction 4 is the dimerization reaction 2 that occurs in the absence of added ligand. Since the rate of this reaction is comparable to the rate at which $\mathbf{3}^+$ is generated, it must be included in the simulations. If it is excluded, the simulated voltammograms display higher reversibility than the experimental data at scan rates fast enough so that no $\mathbf{3}^{+/0}$ couple is visible (>400 mV/s). Other possible scenarios were also considered. The rate-limiting step represented by eq 5 cannot be CO insertion, because the resulting acyl group would be electron-withdrawing from the pyrylium ring and the product's potential would be more positive than that of $\mathbf{1}^+$. Nucleophilic attack on the pyrylium ring could occur at the 2-, 4-, or 6-position, but would result in the formation of a pyran complex, which would be reduced at potentials typical of $Mn(CO)_5R$ species, i.e., <−2 V vs Fc as shown for the dimeric complex **2** discussed earlier. If nucleophilic attack could occur on $\mathbf{1}^0$, then it should be more facile upon $\mathbf{1}^+$, a possibility ruled out by earlier NMR experiments, thereby ruling out the notion that nucleophilic attack on the ring is rate-limiting.

A comparison of Figures 3a (1.3 mM PPh_3) and 3b (13 mM PPh_3) shows that a 10-fold increase in the PPh_3 concentration has very little effect on the CV data. A similar effect can be seen in Figures 4a and 4b for the SWV data. Coordination of PPh_3 must therefore occur after the rate-limiting step since the concentration of PPh_3 has only a minor effect on the amount of $\mathbf{3}^{+/0}$ generated at the electrode surface. Since CO loss must occur at some point in the substitution reaction, we postulate that a slow CO loss from $\mathbf{1}^0$ must form a coordinatively unsaturated intermediate, $(OC)_4MnR$, **4**, which quickly reacts with PPh_3 to form $\mathbf{3}^0$. The CV data are otherwise quite insensitive to mechanism, and several other schemes were found to account for the CV data, but these failed to fit the four sets of SWV data.

To simulate the data in Figure 5, eq 5 has to be reversible, with $k_{-2} \gg k_2$. The value of k_{-2} has little effect on the simulations of CVs and SWVs shown in Figures 3 and 4. The data in Figure 5 allow for a more precise estimation of this parameter because of their longer time scale. These voltammograms were obtained by holding the electrode at a potential sufficiently negative to reduce $\mathbf{1}^+$ for time τ and then rapidly sweeping to positive potentials to analyze the composition of the "cloud" of products generated at the electrode

(24) (a) Osteryoung, J. *Acc. Chem. Res.* **1993**, *26*, 77. (b) O'Dea, J. J.; Wikiel, K.; Osteryoung, J. *J. Phys. Chem.* **1990**, *94*, 3628.

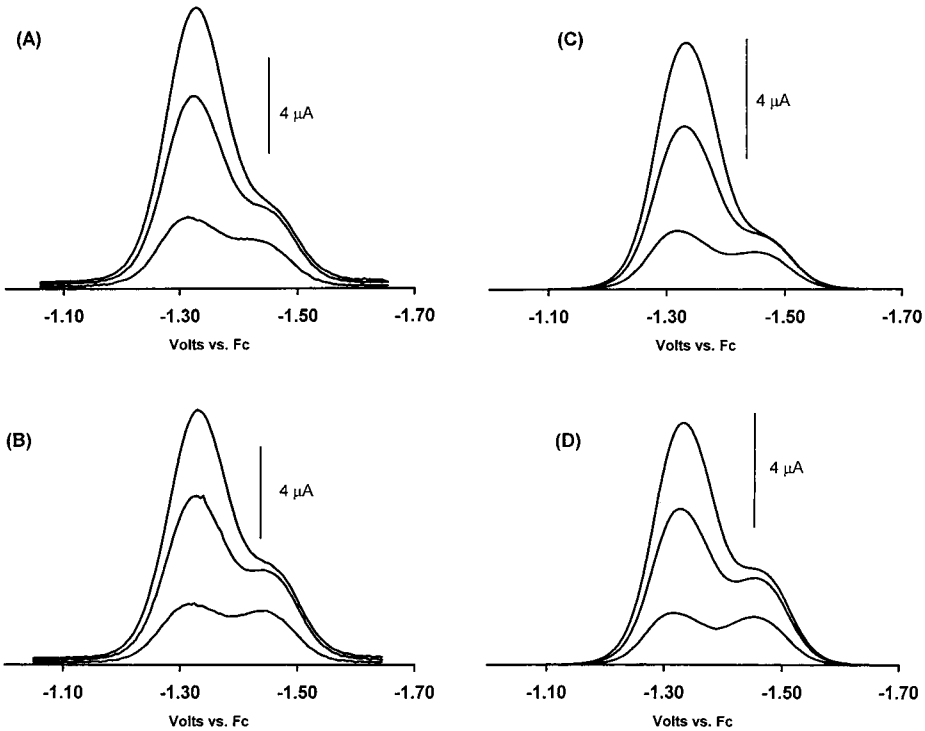

Figure 4. SWVs (pulse width = 5 mV, pulse height = 50 mV) of 1.3 mM **1**BF_4 at 1, 5, and 10 Hz: (A) 1.3 mM PPh_3; (B) 13 mM PPh_3; (C) simulation, 1.3 mM PPh_3; (D) simulation, 13 mM PPh_3.

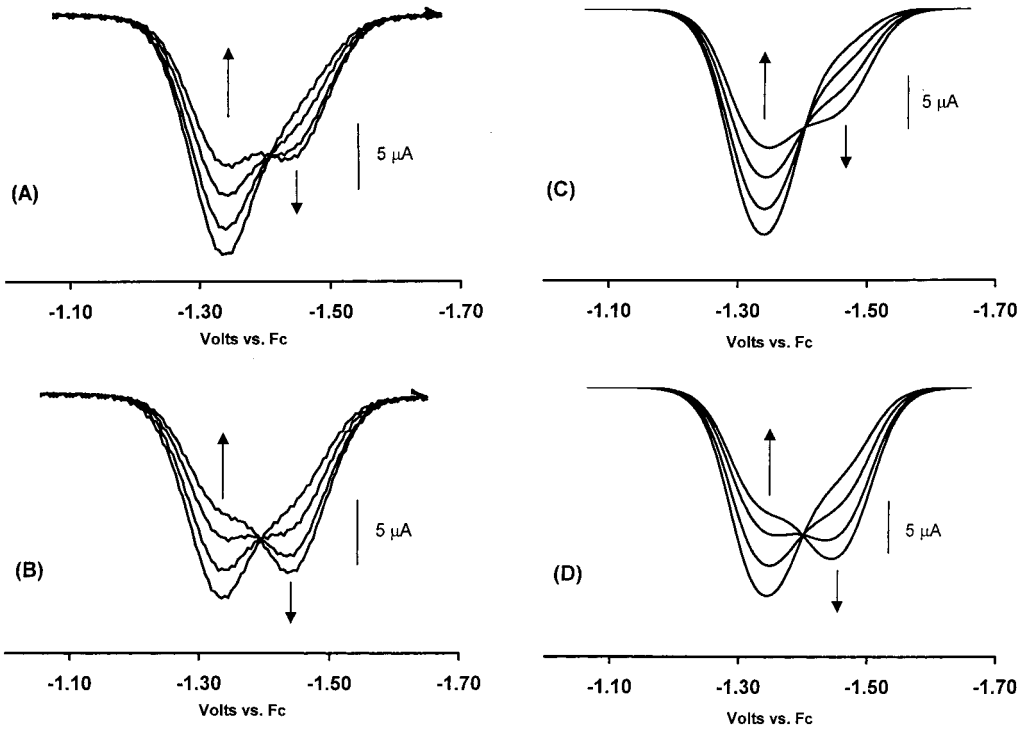

Figure 5. SWVs (pulse width = 2 mV, pulse height = 50 mV, 100 Hz) of 1.3 mM **1**BF_4 where electrode was held at −1.7 V vs Fc for time τ = 1, 2, 4, and 8 s before scan. Arrows indicate trend in peak height with increasing τ: (A) 1.3 mM PPh_3; (B) 13 mM PPh_3; (C) simulation, 1.3 mM PPh_3; (D) simulation, 13 mM PPh_3.

surface. A value of $k_{-2} = 1.0 \times 10^4$ M^{-1} s^{-1} ± 10% was estimated from these data. This value is quite reasonable for a process where a ligand attaches to a 16-electron coordinatively unsaturated species.[25] The equilibrium constant $K = 7 \times 10^{-5}$ for eq 5 can be estimated from k_2 and k_{-2}. This reaction occurs independently of whether PPh_3 is present and must contribute to the lower chemical reversibility of the $\mathbf{1}^{+/0}$ couple observed at slow scan rates at low temperatures and the curvature of the van't Hoff plot for the reduction of $\mathbf{1}^+$ discussed earlier.

Another key observation from the SWV data is that the sum of the cathodic currents due to $\mathbf{1}^{+/0}$ and $\mathbf{3}^{+/0}$ equal the current of $\mathbf{1}^{+/0}$ in the absence of PPh_3. This effect can be seen most clearly in Figure 5. At longer times, more **3** is generated, at the expense of **1** present

at the electrode surface. This observation means that $\mathbf{3}^+$ must be generated by an electrocatalytic mechanism; that is, $\mathbf{1}^+$ is reduced to $\mathbf{1}^\mathbf{0}$, which is quickly converted to **3**. At $E°(\mathbf{1}^{+/0})$, $\mathbf{3}^\mathbf{0}$ is reoxidized at the electrode surface to $\mathbf{3}^+$, resulting in a net decrease in the cathodic current observed for $\mathbf{1}^{+/0}$. When the scan reaches $E°(\mathbf{3}^{+/0})$, the $\mathbf{3}^+$ at the electrode surface is rereduced. The electrocatalysis for this reaction is fairly slow, being limited by the rate of CO dissociation from $\mathbf{1}^\mathbf{0}$. It should be noted that this CO dissociation is 3700 times faster than the CO dissociation observed for $Mn(CO)_5Br$.[26] The SWV data allow for the estimation of the value of k_3 as well. The value of k_{-2} must be larger than k_3 by about a factor of 10; otherwise the simulated signal for $\mathbf{3}^{+/0}$ in Figures 4c and 4d at 10 Hz is smaller than that at 5 Hz. Similarly, the value of k_3 has to be slightly larger than k_2; otherwise the $\mathbf{3}^{+/0}$ signal is too small in all the CVs and SWVs.

Overall, the mechanism described by eqs 3−7 fits the data very well, as shown by the close match between the data and the simulations shown in Figures 3−5. While several other mechanisms were considered, they produced simulations that only fit the data collected by one technique (e.g., CV) at one PPh_3 concentration, often at only one scan rate. For example, a mechanism where PPh_3 substitution occurred via the dimer **2** was ruled out because the reversibilities for the simulated CVs and SWVs at low sweep rates were too high when the data fit high sweep rates. The diffusion coefficients used for these simulations were arbitrarily set at 1.0×10^{-5} cm^2 s^{-1} since, as previously observed by Kochi for the electrocatalytic mechanism, the diffusion coefficient has only a minor effect on the shape of the voltammograms.[27] Indeed, when this parameter was varied by a factor of 10 for any individual species, little change was observed in the simulation thus obtained. Similarly, fast electron-transfer reactions and transfer coefficients of 0.5 were assumed.

The identity of $\mathbf{3}^+$ was probed during a bulk coulometry experiment. A 1.0 mM solution of $\mathbf{1}^+BF_4$ was electrolyzed at −1.2 V vs Fc in the presence of 1.3 mM PPh_3. A total of 0.07 Faraday-equivalents of charge was passed through the solution, which changed from yellow to dark orange during the exhaustive electrolysis. The low charge count confirms the catalytic nature of the ligand substitution process. After electrolysis, a single reversible wave at −1.41 V vs Fc, due to $\mathbf{3}^{+/0}$, was observed and the solution displayed IR bands at 2070, 2024, 2000, and 1971 cm^{-1}. The pattern is consistent with a tetracarbonylmanganese complex which is more electron rich than the starting material $\mathbf{1}^+$.

$\mathbf{3}^+PF_6$ was synthesized by the reaction of 1 equiv of PPh_3 with $\mathbf{1}PF_6$ in DME in the presence of a catalytic amount of Zn dust, and its spectroscopic, microanalytical, and electrochemical properties confirm the assignment made from the electrochemistry.

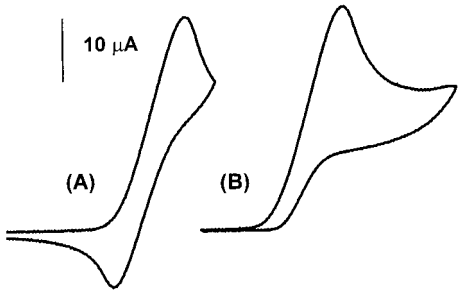

Figure 6. (A) CV of 5.0 mM $\mathbf{1}BF_4$ at 800 mV/s; (B) in the presence of 16.8 mM $HSnPh_3$.

Electrochemistry of $\mathbf{1}^+$ in the Presence of $HSnPh_3$ and Proton Donors. Hydrogen atom abstraction reactions are typical of radicals.[28] It appears that $\mathbf{1}^\mathbf{0}$ may abstract H atoms from $HSnPh_3$ (a known H atom donor)[29] presumably to become one or more pyran complexes designated in eq 9 as "**5**".

Since pyrans are known to act as H^- donors, mild sources of H^+ were added to the cell to see if catalytic H_2 production would occur. The loss of H^- from a pyran complex **5** would regenerate $\mathbf{1}^+$, thereby closing a catalytic cycle as described below.

$$\mathbf{1}^+ + e^- \rightleftharpoons \mathbf{1}^\mathbf{0} \qquad E° = -1.33 \text{ V vs Fc} \tag{8}$$

$$\mathbf{1}^\mathbf{0} + H^\bullet \rightarrow \mathbf{5} \tag{9}$$

$$\mathbf{5} + H^+ \rightarrow \mathbf{1}^+ + H_2 \tag{10}$$

Addition of excess $HSnPh_3$ to solutions of $\mathbf{1}^+$ drastically alters the appearance of the cyclic voltammograms (Figure 6) in both CH_2Cl_2 and THF. The wave is no longer reversible at low scan rates, and the peak potential moves to slightly more positive values. This behavior is consistent with an H atom abstraction process, as is the fact that the wave due to the dimer **2** disappears when the tin hydride is added. If the scan rates are increased or the temperature decreased, the reduction feature becomes more reversible, which indicates that this reaction is not much faster than the dimerization reaction described in eq 4. At high scan rates (>1600 mV/s) and low temperatures (<−20 °C), the voltammograms are indistinguishable from those recorded in the absence of $HSnPh_3$.

When a scan is performed prior to and immediately after the addition of water or a carboxylic acid to a THF solution of $\mathbf{3}^+$ and $HSnPh_3$, a 20% increase in current is observed. The wave also becomes more plateau-shaped. These observations are consistent with mild catalysis at the electrode surface. Unfortunately, subsequent scans show that the complex decomposes under these conditions, with the peak at $E_{pc} = -1.30$ V vs Fc decreasing in intensity over time. Interestingly, the $\mathbf{1}^{+/0}$ couple itself is unaffected by water, mesitol, 2-propanol, or methanol in the absence of $HSnPh_3$ on the CV time

(25) (a) Pearson, J.; Cooke, J. Takats, J. Jordan, R. B. J. Am. Chem. Soc. **1998**, *120*, 1434, and references therein. (b) Boese, W. T.; Ford, P. C. In *Electron-Transfer Reactions*; Isied, S. S., Ed.; American Chemical Society: Washington, 1997; p 221. (c) Poli, R., Owens, B. E.; Linck, R. G. *J. Am. Chem. Soc.* **1992**, *114*, 1302. (d) Peaver, K. A.; Holl, M. M. B.; Carpenter, G. B.; Rieger, A. L.; Rieger, P. H.; Sweigart, D. A. *Organometallics* **1995**, *14*, 512.

(26) Angelici, R. J.; Basolo, F. *Inorg. Chem.* **1963**, *2*, 728.

(27) (a) Zizelman, P. M.; Amotore, C. Kochi, J. K. *J. Am. Chem. Soc.* **1984**, *106*, 3771. (b) Astruc, D. *Electron Transfer and Radical Processes in Transition Metal Chemistry*; VCH Publishers: New York, 1995; Chapter 6.

(28) (a) Trogler W. C. *Organometallic Radical Processes*; Elsevier: New York, 1990. (b) Iqbal, J.; Bhatia, B.; Nayyar, N. K. *Chem. Rev.* **1994**, *94*, 519.

(29) (a) Amatore, C. *J. Org. Chem.* **1996**, *61*, 9402, and references therein. (b) Curran, D. P.; Hadida, S.; Kim, S.-Y.; Luo Z.; *J. Am. Chem. Soc.* **1999**, *121*, 6607, and references therein.

scale. The catalytic increase in current also occurs when chloroacetic acid or phenylacetic acid is added to the solution, thereby indicating that alcohols are not acidic enough to be H^+ donors to the pyran complex.

Preparative attempts to characterize the electrode products have been unsuccessful. Bulk electrolysis of a sample of $\mathbf{1}^+$ at a Pt electrode in the presence of excess $HSnPh_3$ results in the passage of 1-Faraday equivalent of charge, and the neutral products can be extracted from the supporting electrolyte and analyzed by ^1H NMR. This approach indicates that a plethora of products are formed as judged by the 20 or so resonances in the region appropriate for the methoxy group. It is not clear whether these final products result from decomposition of a small number of species initially generated at the electrode. Reaction of $\mathbf{1}^+$ with $HSnPh_3$ or HSnBu with Zn in DME yields results similar to electrolytic preparation. Bulk electrolysis of $\mathbf{1}^+$ in the presence of proton donors at a Hg-pool electrode also leads to complete consumption of the complex with the passage of ca. 1-Faraday equivalent of charge. No gas evolution was observed. While the color changed from yellow to dark orange during electrolysis, the product solution was devoid of IR bands due to metal-carbonyl-containing species.

Conclusions

Complex $\mathbf{1}^+BF_4$ is a surprisingly robust compound, which resists electrophilic Mn−C bond cleavage by H^+ and CO-insertion reactions, but has a rich electrochemistry, which results from the union of a metal complex with a pyrylium ligand. In the absence of coordinating ligands, the complex slowly dimerizes after reduction through the coupling of pyranyl radicals. This coupling produces several isomeric products. After reduction, the complex also appears to undergo a dissociative equilibrium involving loss of CO 3700 times faster than that observed for $Mn(CO)_5Br$. This equilibrium heavily favors the starting material. The coordinatively unsaturated intermediate **4** is rapidly trapped by both CO and PPh_3 to regenerate the starting material or complex **3**, respectively. The CO-dissociation equilibrium constant and the rate constants for the coordination of these two ligands to **4** were estimated through simulations of cyclic voltammetric and square wave voltammetric data, both data sets being necessary to completely discern the kinetics of this reaction. The CO-dissociation process ultimately controls the rate of an electrocatalytic ligand substitution reaction.

On the CV time scale, complex $\mathbf{1}^+$ appears to be involved in a catalysis which involves $HSnPh_3$ and weak acids, presumably to generate H_2. Unfortunately, the electrode products decompose during bulk electrolysis in the presence of protic species, precluding attempts to quantify this electrocatalytic reaction on a preparative scale.

Experimental Section

All reactions and subsequent manipulations involving organometallic reagents were performed under anaerobic and anhydrous conditions in an atmosphere of prepurified dinitrogen or argon. Diethyl ether, hexanes, dichloromethane, and chloroform-*d* were purified by distillation from CaH_2 into 500 mL storage vessels charged with additional CaH_2. THF was distilled from sodium-benzophenone ketyl into a 500 mL storage flask charged with fresh benzophenone ketyl. All solvents were vacuum transferred directly into reaction vessels. Methyl propiolate (Acros), diphenylacetylene (Acros), tetrafluoroboric acid (Acros), cyclopentadienyldicarbonyliron dimer (Aldrich), and dimanganese decacarbonyl (Alfa-Aesar) were obtained commercially and were used as received. $Mn(CO)_5CH_3$[30] and NBu_4PF_6 were prepared as detailed in the literature. NMR spectra were obtained with a 300 MHz Varian 300 Unity Plus spectrometer. IR spectra were obtained using a Mattson Research Series IR spectrophotometer. NMR spectra were obtained on samples prepared in a drybox under an anhydrous atmosphere of argon.

General procedures used for electrochemistry have been described elsewhere. Electrochemical measurements were performed using an EG&G PAR 263 potentiostat interfaced to a computer. Electrodes and cells were obtained from BAS, and a vacuum cell was custom-built by ChemGlass. Bulk electrolysis was performed using a BAS bulk electrolysis cell contained within the vacuum cell. The working electrode was made of reticulated vitreous carbon. Simulations were performed using DIGISIM software available from BAS or ESP 2.4.[24]

Synthesis of $\mathbf{1BF_4}$. $Mn(CO)_5CH_3$ (0.285 g, 1.35 mmol) was dissolved in CH_2Cl_2 (20 mL), and $HBF_4{\cdot}Et_2O$ (54%, 1.86 mL, 1.35 mmol) was added by syringe. The mixture was covered and stirred in the dark for 3 h at 20 °C. Methyl propiolate (0.121 mL, 1.35 mmol) was added by syringe and the mixture stirred in the dark for 10 min. Diphenylacetylene (0.242 g, 1.1 mmol) was added, and the mixture was stirred in the dark for 48 h. The solution was filtered through Celite supported on a porous medium glass frit and concentrated under reduced pressure until the solution volume was ca. 5 mL. About 1 mL of Et_2O was added and the solution cooled to −30 °C overnight. The yellow crystals that formed were isolated by cannulation. Two further crops were obtained for a total yield of 0.15 g (15%). Anal. Calcd: C, 50.77; H, 2.59. Found: C, 51.01; H, 2.61. ^1H NMR ($CDCl_3$) δ: 8.45 (s, 1H, $C_5H(OCH_3)Ph_2$); 7.65−7.28 (m, 10H, *Ph*$_2$) 4.62 (s, 3H, OCH_3). ^{13}C NMR ($CDCl_3$) δ: 60.05 ppm (OCH_3). IR: ν (CO) 2135, 2084, 2040, 2017 cm^{-1}, ν(pyrylium CO) 1630 cm^{-1}. $E^{\circ\prime}(CH_2Cl_2)$: −1.33 V vs Fc. FAB-MS: 457 *m*/*z* ($P^+ - BF_4$).

Synthesis of $\mathbf{1PF_6}$. $Mn(CO)_5Br$ (1.05 g, 3.82 mmol) was dissolved in a CH_2Cl_2 (25 mL) solution of $AgPF_6$ (0.963 g, 3.81 mmol). A yellow precipitate immediately formed, and the mixture was stirred for 30 min at 20 °C. Methyl propiolate (0.56 g mL, 6.66 mmol) was added by syringe and the mixture stirred in the dark for 10 min, whereupon the color of the mixture lightened slightly. Diphenylacetylene (0.68 g, 3.81 mmol) was added, and the mixture was stirred in the dark for 48 h. The solution was filtered through Celite supported on a porous medium glass frit, Et_2O (10 mL) was added, and the solution was concentrated under reduced pressure until its volume was ca. 10 mL. The yellow crystals that formed upon cooling to −30 °C overnight were isolated by cannulation. Two further crops were obtained for a total yield of 0.69 g (30%). Anal. Calcd: C, 45.86; H, 2.34. Found: C, 45.92; H, 2.29. ^1H NMR($CDCl_3$) δ: 8.45 (s, 1H, $C_5H(OCH_3)Ph_2$); 7.65−7.28 (m, 10H, *Ph*$_2$) 4.62 (s, 3H, OCH_3). ^{13}C NMR ($CDCl_3$) δ: 60.05 ppm (OCH_3). IR: ν (CO) 2135, 2084, 2040, 2017 cm^{-1}, ν(pyrylium CO) 1631 cm^{-1}. $E^{\circ\prime}(CH_2Cl_2)$: −1.33 V vs Fc.

Synthesis of $\mathbf{3PF_6}$. $\mathbf{1}PF_6$ (0.088 g, 0.15 mmol) was reacted in DME (10 mL) with PPh_3 (0.038, 0.015 mmol) in the presence of a trace of Zn dust. The yellow solution changed to orange upon stirring overnight. The solvent was removed under reduced pressure and the residue recrystallized from $CHCl_3$/Et_2O. A total of 0.091 g of yellow needles was recovered (74% yield). Anal. Calcd: C, 57.43; H, 3.49. Found: C, 57.33; H, 3.39. ^1H NMR($CDCl_3$) δ: 7.72 (s, 1H, $C_5H(OCH_3)Ph_2$); 7.00−7.55 (m,

(30) McKinney, R. J.; Crawford, S. S. *Inorg. Synth.* **1989**, *26*, 155.

25H, *Ph*,) 4.46 (s, 3H, OCH_3). ^{13}C NMR ($CDCl_3$) δ: 60.02 ppm (OCH_3). IR: ν (CO) 2084, 2084, 2017, 1993 cm^{-1}, ν(pyrylium CO) 1686 cm^{-1}. $E°'$(CH_2Cl_2): −1.43 V vs Fc. Electrospray MS: 691 ($P^+ - PF_6$), 663 ($P^+ - PF_6 - CO$), 635 m/z ($P^+ - PF_6 - 2CO$).

Acknowledgment. This research was supported by a Cottrell College Science Award from Research Corporation (CC5264). We also acknowledge the Department of Chemistry, the College of Arts and Sciences, and the Graduate School of Southern Illinois University Edwardsville, for their continuing financial support. Mass spectrometry was provided by the Washington University Mass Spectrometry Resource, an NIH Research Resource (Grant No. P41RR00954).

OM020405N